Syllabic discrimination in premature human infants prior to complete formation of cortical layers

Mahdi Mahmoudzadeh[a], Ghislaine Dehaene-Lambertz[b,c,d], Marc Fournier[a], Guy Kongolo[a], Sabrina Goudjil[a], Jessica Dubois[b,c,d], Reinhard Grebe[a], and Fabrice Wallois[a,1]

[a]Institut National de la Santé et de la Recherche Médicale (INSERM) U1105, GRAMFC, Université de Picardie Jules Verne, CHU Amiens, F80000 Amiens, France; [b]INSERM U992, Cognitive Neuroimaging Unit, F91191 Gif-sur-Yvette, France; [c]Commissariat à l'Energie Atomique, NeuroSpin, F91191 Gif-sur-Yvette, France; and [d]Université Paris XI, F91405 Orsay, France

Edited by Patricia Kuhl, University of Washington, Seattle, WA, and approved January 22, 2013 (received for review July 19, 2012)

The ontogeny of linguistic functions in the human brain remains elusive. Although some auditory capacities are described before term, whether and how such immature cortical circuits might process speech are unknown. Here we used functional optical imaging to evaluate the cerebral responses to syllables at the earliest age at which cortical responses to external stimuli can be recorded in humans (28- to 32-wk gestational age). At this age, the cortical organization in layers is not completed. Many neurons are still located in the subplate and in the process of migrating to their final location. Nevertheless, we observed several points of similarity with the adult linguistic network. First, whereas syllables elicited larger right than left responses, the posterior temporal region escaped this general pattern, showing faster and more sustained responses over the left than over the right hemisphere. Second, discrimination responses to a change of phoneme (ba vs. ga) and a change of human voice (male vs. female) were already present and involved inferior frontal areas, even in the youngest infants (29-wk gestational age). Third, whereas both types of changes elicited responses in the right frontal region, the left frontal region only reacted to a change of phoneme. These results demonstrate a sophisticated organization of perisylvian areas at the very onset of cortical circuitry, 3 mo before term. They emphasize the influence of innate factors on regions involved in linguistic processing and social communication in humans.

hemodynamic response | premature human brain | language | hemispheric lateralization | near infrared spectroscopy

Shortly after birth, human infants already exhibit a variety of sophisticated linguistic capacities, from discriminating syllables and human languages (1) to remembering short stories (2). These capacities rely on a set of perisylvian brain areas similar to the one described in adults, involving temporal but also frontal areas (3), with significant asymmetries favoring the left hemisphere at the level of the *planum temporale* (4, 5). Because audition is already functional during the last months of pregnancy (6), it is still debated whether evolution has endowed humans with a genetically determined cortical organization particularly suitable to process speech or whether fast learning quickly specializes the auditory network toward speech processing during this initial period (7). In the present work, to inform this debate, we examined the functional organization of the perisylvian areas at the onset of cortical circuitry in preterm infants.

Neuronal migration is still on its way during the last trimester of human gestation. The majority of the neurons still lie in the subplate, and the six-layered lamination of the cortex becomes fully visible only after 32-wk gestational age (wGA) (8). The first contacts of the thalamo-cortical fibers establish with subplate neurons (9). The first synapses appear in the cortical plate around 26 wGA, with a massive relocation of the afferent fibers from the subplate to the cortical plate from 28 to 32 wGA. A dual innervation of pyramidal cells by both subplate and thalamic axons is thus present (10), creating a transient circuitry for incoming inputs, very specific to this period of development. This period is also marked by a fast emergence of short-range connectivity in addition to the long-range association pathways already observed (11). Auditory event-related responses to tones have been recorded from 25 wGA onward (12). Although the cortical origin of these early event related potentials (ERPs) is debatable, a clear cortical response to external sounds has been detected with functional MRI (fMRI) at 33 wGA in fetuses (13).

To probe the functional efficacy of the early cortical circuitry in processing speech stimuli, we examined a linguistic (ba vs. ga) and a nonlinguistic (male vs. female voice) discrimination in 12 sleeping 30 wGA preterm infants (28–32 wGA; Table S1). Beyond their linguistic/nonlinguistic valency, these two contrasts differ on acoustical properties that can affect their discriminability and their processing by the left and right hemisphere. A place of articulation contrast, such as ba/ga, is one of the most challenging phonetic discriminations, easily lost in degraded hearing conditions (14, 15). Its perception requires a fine-grained temporal analysis and mainly relies on a left-lateralized network both in adults (16, 17) and in infants (18, 19). By contrast, the perception of a change in voice sex is based on spectral differences carried by the whole syllable and better processed by the right temporal regions (20–23). The comparison of cortical responses to these two contrasts should clarify whether a sophisticated phonetic discrimination and a simpler acoustic discrimination occur at the same moment in development and whether the delay observed in the anatomical gyration of the left hemisphere has functional consequences for speech processing. Indeed, most sulci, particularly the superior temporal sulcus (STS), appear 1 or 2 wk later on the left than on the right hemisphere (24, 25). This might lead to differences in their respective capacities to encode and discriminate auditory stimuli.

Because it is ethically problematic to move preterm infants to a brain-imaging unit, we used functional near-infrared spectroscopy (fNIRS) to test them at bedside. Oxy- (HbO) and deoxy-hemoglobin (Hb) absorb light specifically at different wavelengths. It is thus possible to measure changes in their concentration in the vessels surrounding a neurally active region and to infer the neural response to external stimuli in the cortex coarsely located between a light emitter and a detector placed on the scalp (26). Here, we used 10 measurement channels placed above the perisylvian areas of each hemisphere and a block design (20 s of stimulation followed by 40 s of silence) to present syllables organized in three types of blocks (Fig. 1). In standard blocks (ST), all syllables were identical. In deviant blocks, 15% were different, either beginning with another consonant in deviant phoneme blocks (DP) or

Author contributions: G.D.-L., G.K., S.G., and F.W. designed research; M.M. and F.W. performed research; M.M. and J.D. contributed new reagents/analytic tools; M.M., G.D.-L., M.F., and R.G. analyzed data; and M.M., G.D.-L., and F.W. wrote the paper.

The authors declare no conflict of interest.

This article is a PNAS Direct Submission.

Freely available online through the PNAS open access option.

[1]To whom correspondence should be addressed. E-mail: fabrice.wallois@u-picardie.fr.

This article contains supporting information online at www.pnas.org/lookup/suppl/doi:10.1073/pnas.1212220110/-/DCSupplemental.

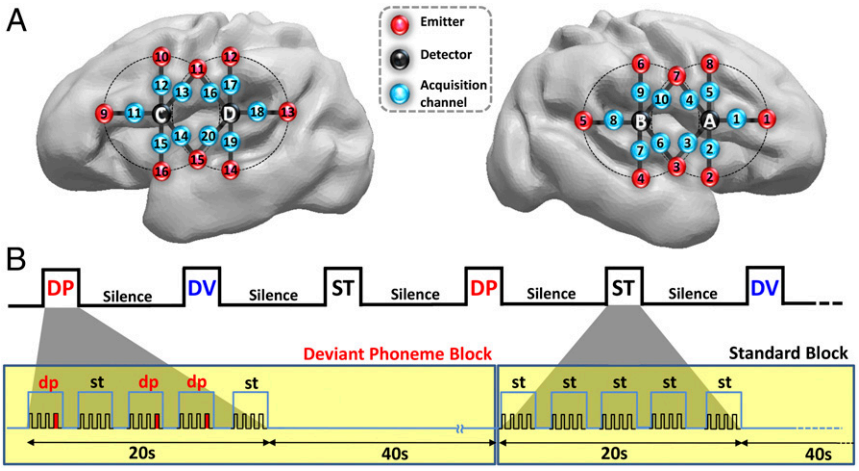

Fig. 1. (*A*) Estimated projection of the optodes (channels 1–10: right hemisphere; channels 11–20: left hemisphere) on the brain of a 30 wGA preterm infant (Fig. S1). (*B*) Experimental paradigm, deviant phoneme (DP), deviant voice (DV), and standard (ST) blocks (*Materials and Methods*).

changing in voice sex in deviant voice blocks (DV). Repetition of the same stimulus classically produces a decrease in neural activity, whereas a sudden change causes a recovery of the neural activity in regions coding the parameter that changed (18, 27). This recovery, or mismatch response, affects the amplitude and temporal characteristics (i.e., slope and latency to the peak) of the hemodynamic response in adults (28–30) and infants (3, 22). We thus expected a weaker amplitude and slower response in standard blocks relative to deviants blocks if preterms perceive the change of stimulus (22). We tested amplitude differences between experimental conditions first with cluster-based statistics considering each time bin and channel and second with an ANOVA on the area under the curve (AUC) to reveal the channels with the most robust and sustained differences. Then we evaluated the response dynamics in each condition by determining its significant onset relative to baseline in each channel and its global slope in each hemisphere. Because these analyses suggested a transient response for the deviant voice condition not captured by the previous analyses, we reexamined the amplitude differences while focusing on the first 6 s of stimulation (i.e., during the rising edge of the hemodynamic response).

Results

Hemodynamic Responses to Speech in Preterms' Perisylvian Regions. The neuro-vascular coupling already described in premature infants (31) was sufficiently mature to track brain responses to our stimulation paradigm in bilateral perisylvian channels. HbO increased and Hb decreased shortly after auditory stimulation, with a time course similar to full-term infants and adults (3, 32), peaking ~5–7 s after the stimulus onset (Movie S1; Fig. S2). We focused our analyses on the HbO signal, whose signal-to-noise ratio is better than Hb, and used cluster-based statistics to probe asymmetries in the responses to all conditions merged together. The responses were mostly right lateralized as established by a larger right than left amplitude in a suprasylvian and in a temporal cluster of channels (ch): ch 1, 4, 5, 9, and 10 (5–23 s; $P_{\text{cluster-cor}} = 0.0002$) and ch 2, 3, 6, and 7 (6–25 s; $P_{\text{cluster-cor}} = 0.0005$). However, a left-hemispheric lateralization was observed over the posterior temporal and supramarginal regions: on these channels, the response started earlier [ch 4 and 6–10 (1–11 s); $P_{\text{cluster-cor}} = 0.005$], and the final undershoot was less pronounced [ch 6–9 (15–25 s); $P_{\text{cluster-cor}} = 0.002$] on the left than on the right hemisphere (Fig. 2).

Phoneme and Voice Changes Elicit Different Responses. We then examined the HbO responses to deviant stimuli. The hemodynamic response in the DP condition was faster, larger, and lasted longer in almost all channels relative to ST (Fig. 3; Movie S1). Cluster-based statistics included all channels into a single cluster within each hemisphere, significant for the entire duration of the analyzed segment (2–24 s; right: $P_{\text{cluster-cor}} < 0.0001$; left: $P_{\text{cluster-cor}} = 0.0005$; Fig. 3). The analysis of the AUC confirmed that the discrimination response was significant in left supramarginal ch 17–18, left frontal ch 12, and right posterior temporal ch 7 ($P_{\text{cor}} < 0.003$; Figs. S3 and S4 for individual responses).

This robust response to a change of phoneme stood in sharp contrast to the response to a change of voice. Deviant-voice blocks elicited a significantly weaker and shorter response than standard blocks [right hemisphere cluster: ch 1–10 (8–17 s); $P_{\text{cluster-cor}} = 0.003$; left temporal cluster: ch 14, 15, and 20 (7–16 s), $P_{\text{cluster-cor}} = 0.023$; frontal/central cluster: ch 12, 13, and 16 (10–23 s); $P_{\text{cluster}} = 0.017$; Fig. 3; Figs. S5–S7], except over the left temporal and supramarginal regions where the sharp decrease of the signal at the end of the ST blocks was not observed in DV blocks [ch 14 and 17–20 (15–25 s); $P_{\text{cluster-cor}} = 0.011$]. The AUC analysis revealed a significant difference only in one channel (left temporal ch15) corresponding to a weaker response for DV than for ST. Thus, phonemic and voice changes elicited different responses in preterm brains. This difference between deviant blocks was confirmed by the direct comparison of DP vs. DV conditions which identified two significant clusters [all right channels (2–20 s); $P_{\text{cluster-cor}} = 0.0002$; left suprasylvian ch 11–13 and 16–18 (2–23 s); $P_{\text{cluster-cor}} = 0.0027$; Fig. S5] and by the AUC analysis showing significant differences for ch 7, 9, 15, 17, and 18 ($Ps_{\text{cor}} < 0.003$; Fig. S3).

Dynamics of the Hemodynamic Response. Stimulus repetition generally causes a decrease in neural activity, whereas change elicits a signal recovery (3, 22, 28–30, 33). As deviant blocks always began with a deviant trial, we expected a boost in neural activity due to the novel stimulus and therefore a higher metabolic demand from the earliest seconds of stimulation. This hypothesis was confirmed by a steeper slope for DV and DP relative to ST over the right hemisphere ($P = 0.002$; Fig. 4*C*), but only for DP relative to ST ($P = 0.005$) over the left. Over the right hemisphere, the first significant increase of HbO over the baseline level was ~2.5/3.8 s for the DP/DV vs. 6.9 s for the ST condition, but ~1.7 (DP) vs. 7.9/8.3 s for DV/ST over the left hemisphere (Fig. 4 *A* and *B*).

These analyses thus showed similar initial dynamics for both deviant conditions over the right hemisphere, suggesting a transient positive response to novelty even in the DV condition. This response might have been missed by our previous amplitude analyses that integrated over the whole block. We therefore reanalyzed the amplitude of the activation during the first 6 s of stimulation. We observed a larger response for DP vs. ST in

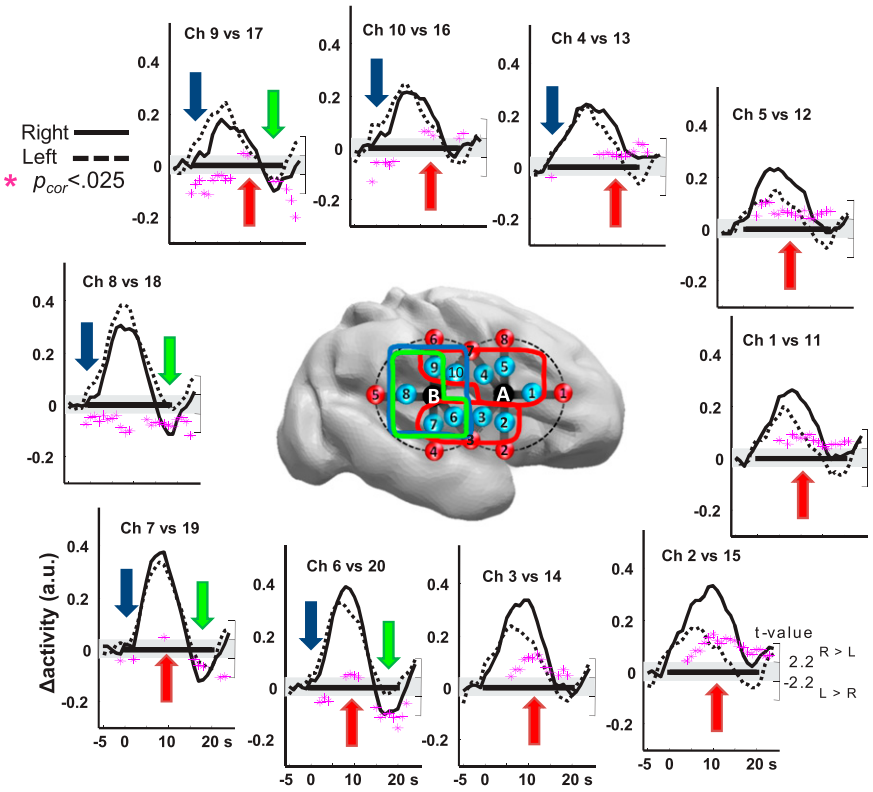

Fig. 2. Functional asymmetry to speech sounds in premature infants. The right and left grand average HbO responses to all conditions are plotted for symmetrical channels, whose locations are presented over a right hemisphere view of a preterm brain. The black rectangle along the *x* axis indicates the duration of the stimulation block (0–20 s). Pink stars indicate the *t*-value of the samples (right scale) included in significant clusters ($P_{cor} < 0.025$). Values are positive when right > left and negative for the opposite direction. The four significant temporo-spatial clusters are identified by colored arrows on the plots and lines surrounding the channels on the brain. Responses are larger on the right hemisphere (red clusters) but are faster (blue cluster) and last longer (green cluster) in the posterior left regions.

channels similar to the above AUC analysis (left ch 12–13 and 16–18 and right ch 2 and 7; $P < 0.002$), confirming the early modulation of the activation by the perception of a phonemic change. For DV, a significant response was observed only in the right frontal ch 5 (DV vs. ST, $P_{cor} = 0.0002$; DP vs. ST, $P_{cor} = 0.009$; DP vs. DV, not significant). The right frontal region thus appeared sensitive to both types of changes, whereas its homologous left region only reacted to a change of phoneme (ch 12: DV vs. ST, not significant; DP vs. ST, $P_{cor} = 0.0005$; DP vs. DV, $P_{cor} = 0.005$; Fig. 3). This pattern yielded a significant hemisphere (ch 5 and 12) × condition (DP and DV) interaction ($P_{cor} = 0.004$).

Discrimination Responses Are Present from 29 wGA Onward. Finally, we examined the stability of the responses in our age range from 28 to 32 wGA (Fig. 3; Fig. S7; Table S2). There was no significant correlation between age and the differences between conditions, either on the first 6 s of stimulation or over the entire block and no difference in the discrimination responses between the six youngest (mean age at test, 29w4d GA) and the six oldest infants (31w6d GA) using cluster-based statistics. Furthemore, most previous analyses were replicated in the youngest group. These babies reacted to a change of phoneme [e.g., analysis of the first 6 s DP vs. ST: main effect of condition: $F(1,5) = 14.6$, $P = 0.012$; condition × channel: $F(9,45) = 6.57$, $P < 0.0001$] and used the left inferior frontal region to detect the change of phoneme [ch 12: DP vs. ST, $F(1,5) = 10.8$, $P = 0.022$]. The response to a change of voice was also congruent with the general results. The condition × channel interaction was significant [$F(9,45) = 3.72$, $P = 0.001$], although not the main effect of condition [$F(1,5) < 1$]. The right inferior frontal region reacted to a change of voice [ch 5: DV vs. ST, $F(1,5) = 8.15$, $P = 0.036$], yielding a significant hemisphere × condition interaction [ch 5 vs. 12 × DP vs. DV: $F(1,5) = 7.9$, $P = 0.037$]. As expected, the same results were observed in the oldest group (Table S2).

Discussion

Our results demonstrate that the human brain, at the very onset of the establishment of a cortical circuit for auditory perception, already discriminates subtle differences in speech syllables. At this point in brain development, the majority of the neurons have not yet reached their final location, and their connectivity is still developing. Nevertheless, the early discrimination network is not limited to auditory areas but already involves inferior frontal regions.

Earlier research already established that the left inferior frontal region, one of the key regions of the adult linguistic network, is already active during speech perception in postterm infants (3, 34). However, it was suggested that its involvement might be secondary to infant's first vocal productions (35, 36). The present results refute this interpretation: preterm infants at this age do not vocalize, and due to their clinical and immature condition, the present participants were not orally fed during their first days of life and were often intubated, restricting their orosensory experience. The early involvement of frontal regions in the speech network might rather represent the functional counterpart of the genetic homogeneity of the "speech regions" revealed by transcriptome analyses during midfetal life. Gene expression in the inferior frontal regions is more similar to other temporal and parietal speech areas than to other frontal areas (37). Leroy et al. (34) observed a correlation in the maturation of the inferior frontal region (area 44), the posterior temporal region, and the arcuate fasciculus during the first weeks of life. These results suggest that the superior temporal,

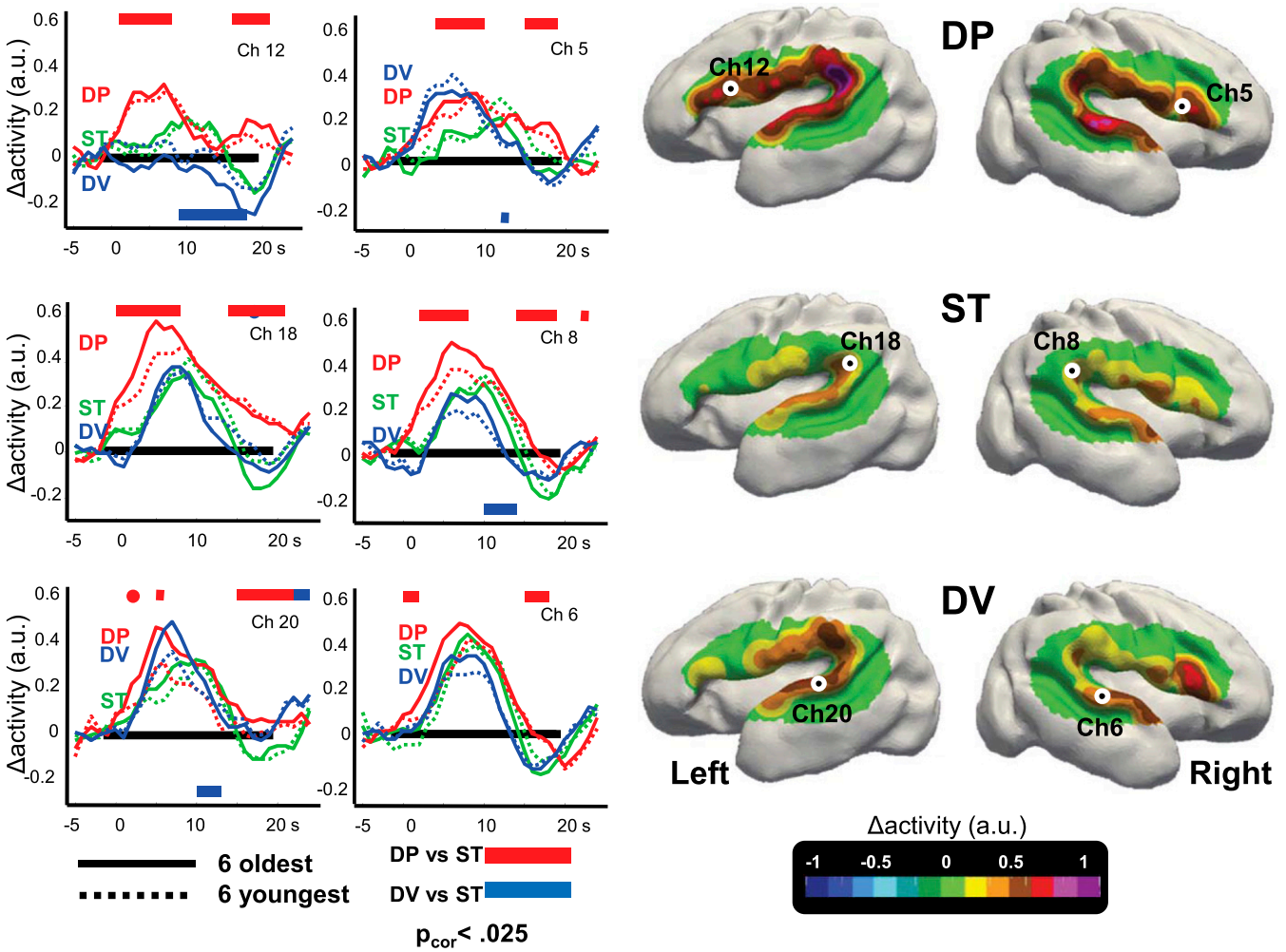

Fig. 3. Discriminative responses to auditory stimuli in premature infants. (*Right*) Surface-based topographic color map of the HbO response at the peak of the hemodynamic response for the three conditions. (*Left*) HbO time courses for the youngest and oldest subsets of six infants, recorded over left Broca's area (ch 12), left *planum temporale* (ch 18), left superior temporal gyrus (ch 20), and their counterlateral right channels (ch 5, ch 8, and ch 6, respectively). The colored rectangles indicate the time windows during which the deviant conditions differ significantly from the standard condition using cluster-based statistics over the whole group. The direction of the effect is given by the location of the bar under or above the *x*-line. Preterm infants discriminate the change of phoneme, notably in the left inferior frontal region. This effect was stable across our age range (28–32 wGA).

inferior parietal, and inferior frontal regions, although distributed across three lobes, belong to a single functional unit.

A phoneme-sensitive cortical network was functional even in our younger infants and remained stable during the investigated time range (Fig. 3). Although we cannot certify that during the 3 d separating birth from the testing day, the environment did not trigger a very rapid development of cortical circuitry, one should remember that these infants were in an extremely precarious condition in an incubator in an intensive care unit and thus had limited contact with the human vocal environment. Peña et al. (38, 39) further demonstrated that preterms do not benefit from their additional exposure to speech, because the first stages of language acquisition are determined by postterm maturational age rather than by the duration of extrauterine life. As is the case for other complex ecological capacities in immature animals, the sophisticated organization of human perisylvian cortex thus appears driven by genetic factors more than by environmental exposure. In rats, for example, a rudimentary neural system for spatial orientation is observed in pups before their first exploration of the environment (40). Newly hatched and thus visually naïve chickens prefer stimuli with a natural biological motion (41). Similarly, phonetic discrimination appears to be part of the early endowment of a human brain. Further work should examine whether this discrimination capacity is shared with other immature mammals or specific to the human lineage.

By contrast with the classical hemodynamic response induced by a novel phoneme, the response to voice deviants was observable only as a fast response, notably over the right hemisphere, which rapidly faded significantly below the standard level after 7 s. This result was unexpected. The voice difference is based on larger acoustic differences than the phonetic contrast, and it was previously shown that preterms discriminate a change in tone frequency (6) and thus encode auditory spectral properties useful for voice perception. One possibility is that we missed the most anterior part of the right superior temporal region, a site of voice discrimination in adults (20) and infants (22, 23), as well as insula and subcortical structures inaccessible to our technique. Neural inhibition or vascular steal from these regions might explain the secondary decrease of the HbO signal significantly below the ST response. Further studies with more extensive recording locations and other brain-imaging techniques are necessary to understand whether these hemodynamic differences might reflect a different efficiency of preterm infants in processing voices and phonemes. In any case, the significant differences we recorded here between

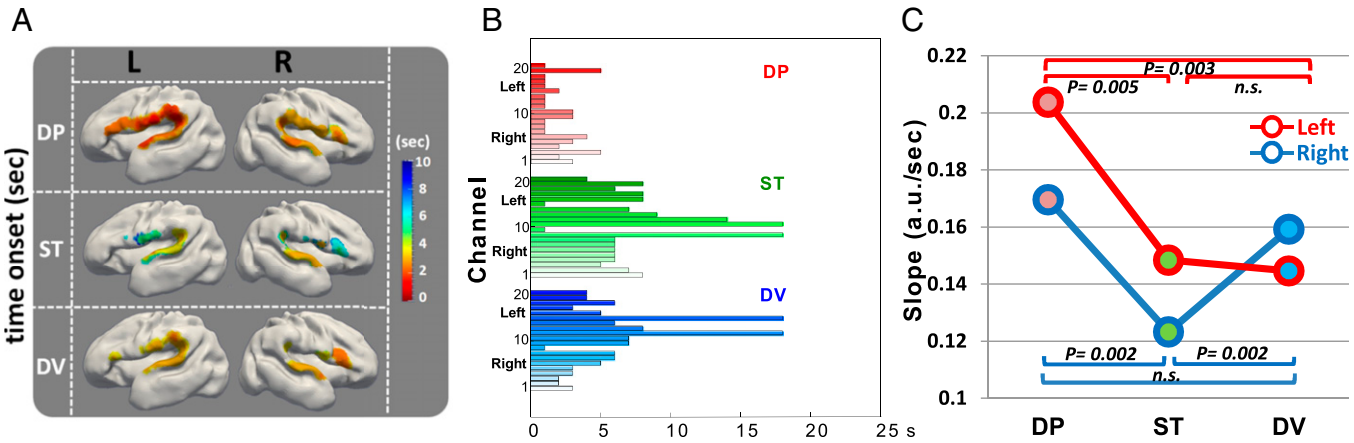

Fig. 4. Dynamics of the HbO response. Topographic map (*A*) and bar plot (*B*) showing the latency of the first significant change in HbO relative to baseline in the different conditions. (*C*) Slope of the HbO response computed across all channels for each condition and hemisphere. The responses to both deviant conditions are faster than ST over the right hemisphere. Over the left hemisphere, only the DP condition is significantly different from the ST condition.

both deviant conditions highlight the functional regionalization already present in the preterm infant's cortex. In that respect, the difference in frontal activation is particularly striking. The left frontal region reacted solely to a phoneme change whereas the controlateral right frontal region reacted to both changes, suggesting that it acts as a generic novelty detector as previously observed in infants (4) and adults (42).

This asymmetry in frontal activation provides additional evidence for an early hemispheric differentiation in humans. Many sulci appear 1 or 2 wk earlier on the right than on the left side (24, 43). Furthermore, cerebral blood flow at rest is larger (44) and the EEG power is higher (45) in the right hemisphere relative to the left before term. These results are congruent with the largest amplitude of the right responses recorded here over most of the channels (Fig. 2). In this context, the reverse asymmetry over the posterior region is noteworthy but congruent with the same left hemisphere bias repeatedly reported at the level of the *planum temporale* in infants for speech stimuli (3–5, 22) but not for music (22, 46). This functional asymmetry cannot be explained by a different distance between our sensors and the brain: we measured no left–right asymmetries in distance at these posterior sites (*SI Text*). The nature of the left-hemispheric functional advantage for speech processing in the posterior temporal region needs to be further explored, but the left–right difference in response speed observed here might suggest faster processing in the left auditory associative areas, allowing a better temporal sampling of auditory input and thus particularly adapted to the fast formant transitions present in speech (4, 16).

To conclude, our results reveal an early organization of the immature human brain into functions useful for deciphering the speech signal. Seventy-six percent of human genes are expressed in the fetal brain from 18 to 23 wGA, and 44% of these are differentially regulated (37). This genetic complexity might endow the human brain with the early functional competences observed here. Although our research demonstrates that brain networks sensitive to phonemes and voices are present at the very onset of cortical organization in humans, it does not challenge the fact that experience is also crucial for their fine tuning and for learning the specific properties of the native language.

Materials and Methods

Participants. Twelve healthy preterm neonates (mean GA at birth, 30.3 ± 1.6 wGA) were tested asleep (recording age, 3.4 ± 1.2 d, corresponding to 30.7 ± 1.5 wGA). All infants had normal auditory and neurological clinical evaluations and were considered at low risk for brain damage (see details in Table S1). Parents were informed of the study and provided their written informed consent. The study was approved by the local ethics committee (Comité Pour la Protection des Personnes Nord-Ouest II).

Experimental Paradigm and Data Recording. Four digitized syllables /ba/ and /ga/, naturally produced by a French male (ba^m, ga^m) and a French female speaker (ba^f, ga^f), were matched for intonation, intensity, total duration (285 ms), prevoicing, and voiced formant transition duration (40 and 45 ms, respectively). These stimuli, used in a previous ERP experiment, induce discrimination responses in 4-mo-old full-term infants (47).

The syllables were presented in series of four (stimulus onset synchrony = 600 ms) to form three types of trials (standard, deviant voice, and deviant phoneme trials). In standard trials, the same syllable was repeated four times (e.g., ga^m ga^m ga^m ga^m). In deviant trials, the last syllable changed relatively to the first three either along the voice dimension (e.g., ga^m ga^m ga^m ga^f), or along the phonetic dimension (e.g., ga^m ga^m ga^m ba^m). Three types of block were constituted and presented randomly, separated by 40 s of silence for a total duration of 108 min (Fig. 1). Each block (duration 20 s) comprised five trials separated by an intertrial interval of 1,600 ms. In standard blocks (ST), all trials were standard trials. Deviant blocks always began with a deviant trial, and then two standard and two deviant trials were randomly intermixed. Deviant trials were along the voice dimension in DV blocks and along the phonetic dimension in DP blocks. In each block, the repeated syllable was kept constant and was randomly chosen among the four possible syllables (ba^m, ga^m, ba^f, and ga^f) to present each syllable the same number of times in each condition and infant.

The infants were tested asleep at night to avoid the day light and the intense day activity of a neonatal care unit. Stimuli were presented at a comfortable hearing level (~70 dB) via speakers placed at the infant's feet, and brain responses were measured with a multichannel frequency domain–based optical imaging system (Imagent; ISS). A special probe made from soft and flexible foam was smoothly secured relatively to anatomical markers to cover the left and right perisylvian areas, providing 10 recording points on each side (see *SI Text* for more details on the recording system).

Data Processing and Statistical Analyses. After converting signal intensities in Hb/HbO concentrations, artifacted blocks were rejected (z-score > 4 in any channel and time sample). The remaining data were band-pass filtered (0.03–0.5 Hz) and segmented relative to the onset of each block (−5 to +25 s). After a linear detrend and a baseline correction were applied, the segments were averaged by condition and channel in each subject (average number of blocks per condition: 19, 19, and 21 for ST, DV, and DP, respectively).

Statistical analyses were performed on the amplitude of the HbO signal (see *SI Text* for complete details on the analyses). Experimental conditions (left vs. right responses, ST vs. DP, ST vs. DV, DV vs. DP) were compared by using two-tailed t tests on the considered variable. A total of 4,096 (2^{12} subjects) random permutations of the original conditions were performed to establish the permutation P value for each comparison. To control the risk of false positive due to multiple comparisons, we either used cluster-based statistics as implemented in the Fieldtrip Matlab toolbox (48), or we corrected the permutation P value by the number of measures done in the considered analysis following the Holm's procedure.

Our statistical approach was as follows. First, we used cluster-based statistics on the 30 time bins × 20 channels to automatically identify, without prior hypotheses, spatial and temporal clusters showing a significant difference

between experimental conditions. Second, to circumscribe our effects to their main spatial location, we reduced the HbO response in each channel and condition to the AUC. Third, to study the dynamics of the response, we evaluated the latency of the first of two samples showing a significant amplitude increase relative to baseline in each condition and channel. We completed this analysis by an analysis of the slope of the HbO signal averaged across all channels of each hemisphere. Because this analysis revealed significant differences between standard and deviant blocks, we next focused on the signal averaged on the first 6 s of the blocks. Finally, to evaluate a potential effect of maturation during our age range, we separated our group in two subsets of six infants, younger and older than 31 wGA at birth (mean age at test, 29w4d vs. 31w6d GA), and looked for differences between these two subgroups in the DP vs. ST and DV vs. ST comparisons using cluster-based analyses. To question the precocity of these discrimination responses, we also performed the same analyses as above, restricted to the younger group.

ACKNOWLEDGMENTS. We thank Petra Huppi for providing preterm MRI data. This work was supported by the *Picardie* regional council.

1. Mehler J, et al. (1988) A precursor of language acquisition in young infants. *Cognition* 29(2):143–178.
2. DeCasper AJ, Spence MJ (1986) Prenatal maternal speech influences newborn's perception of speech sounds. *Infant Behav Dev* 9(2):133–150.
3. Dehaene-Lambertz G, et al. (2006) Functional organization of perisylvian activation during presentation of sentences in preverbal infants. *Proc Natl Acad Sci USA* 103(38): 14240–14245.
4. Dehaene-Lambertz G, Dehaene S, Hertz-Pannier L (2002) Functional neuroimaging of speech perception in infants. *Science* 298(5600):2013–2015.
5. Peña M, et al. (2003) Sounds and silence: An optical topography study of language recognition at birth. *Proc Natl Acad Sci USA* 100(20):11702–11705.
6. Draganova R, et al. (2005) Sound frequency change detection in fetuses and newborns, a magnetoencephalographic study. *Neuroimage* 28(2):354–361.
7. Elman JL, et al. (1996) *Rethinking Innateness: A Connectionist Perspective on Development* (MIT Press, Cambridge, MA).
8. Kostović I, Judas M, Petanjek Z, Simić G (1995) Ontogenesis of goal-directed behavior: Anatomo-functional considerations. *Int J Psychophysiol* 19(2):85–102.
9. Moore AR, Zhou WL, Jakovcevski I, Zecevic N, Antic SD (2011) Spontaneous electrical activity in the human fetal cortex in vitro. *J Neurosci* 31(7):2391–2398.
10. Kanold PO, Luhmann HJ (2010) The subplate and early cortical circuits. *Annu Rev Neurosci* 33:23–48.
11. Takahashi E, Folkerth RD, Galaburda AM, Grant PE (2012) Emerging cerebral connectivity in the human fetal brain: An MR tractography study. *Cereb Cortex* 22(2): 455–464.
12. Rotteveel JJ, de Graaf R, Stegeman DF, Colon EJ, Visco YM (1987) The maturation of the central auditory conduction in preterm infants until three months post term. V. The auditory cortical response (ACR). *Hear Res* 27(1):95–110.
13. Jardri R, et al. (2008) Fetal cortical activation to sound at 33 weeks of gestation: A functional MRI study. *Neuroimage* 42(1):10–18.
14. Miller GA, Nicely PE (1955) An analysis of perceptual confusions among some English consonants. *J Acoust Soc Am* 27(2):338–352.
15. Kraus N, et al. (1996) Auditory neurophysiologic responses and discrimination deficits in children with learning problems. *Science* 273(5277):971–973.
16. Zatorre RJ, Belin P (2001) Spectral and temporal processing in human auditory cortex. *Cereb Cortex* 11(10):946–953.
17. Dehaene-Lambertz G, et al. (2005) Neural correlates of switching from auditory to speech perception. *Neuroimage* 24(1):21–33.
18. Dehaene-Lambertz G, Dehaene S (1994) Speed and cerebral correlates of syllable discrimination in infants. *Nature* 370(6487):292–295.
19. Dehaene-Lambertz G, Baillet S (1998) A phonological representation in the infant brain. *Neuroreport* 9(8):1885–1888.
20. Belin P, Zatorre RJ, Lafaille P, Ahad P, Pike B (2000) Voice-selective areas in human auditory cortex. *Nature* 403(6767):309–312.
21. Bristow D, et al. (2009) Hearing faces: How the infant brain matches the face it sees with the speech it hears. *J Cogn Neurosci* 21(5):905–921.
22. Dehaene-Lambertz G, et al. (2010) Language or music, mother or Mozart? Structural and environmental influences on infants' language networks. *Brain Lang* 114(2): 53–65.
23. Blasi A, et al. (2011) Early specialization for voice and emotion processing in the infant brain. *Curr Biol* 21(14):1220–1224.
24. Chi JG, Dooling EC, Gilles FH (1977) Gyral development of the human brain. *Ann Neurol* 1(1):86–93.
25. Dubois J, et al. (2008) Primary cortical folding in the human newborn: An early marker of later functional development. *Brain* 131(Pt 8):2028–2041.
26. Aslin RN (2012) Questioning the questions that have been asked about the infant brain using near-infrared spectroscopy. *Cogn Neuropsychol* 29(1-2):7–33.
27. Ulanovsky N, Las L, Nelken I (2003) Processing of low-probability sounds by cortical neurons. *Nat Neurosci* 6(4):391–398.
28. Kruggel F, von Cramon DY (1999) Temporal properties of the hemodynamic response in functional MRI. *Hum Brain Mapp* 8(4):259–271.
29. Dehaene-Lambertz G, et al. (2006) Functional segregation of cortical language areas by sentence repetition. *Hum Brain Mapp* 27(5):360–371.
30. Sigman M, Jobert A, Lebihan D, Dehaene S (2007) Parsing a sequence of brain activations at psychological times using fMRI. *Neuroimage* 35(2):655–668.
31. Roche-Labarbe N, Wallois F, Ponchel E, Kongolo G, Grebe R (2007) Coupled oxygenation oscillation measured by NIRS and intermittent cerebral activation on EEG in premature infants. *Neuroimage* 36(3):718–727.
32. Telkemeyer S, et al. (2009) Sensitivity of newborn auditory cortex to the temporal structure of sounds. *J Neurosci* 29(47):14726–14733.
33. Thierry G, Ibarrola D, Démonet JF, Cardebat D (2003) Demand on verbal working memory delays haemodynamic response in the inferior prefrontal cortex. *Hum Brain Mapp* 19(1):37–46.
34. Leroy F, et al. (2011) Early maturation of the linguistic dorsal pathway in human infants. *J Neurosci* 31(4):1500–1506.
35. Kujala A, et al. (2004) Speech-sound discrimination in neonates as measured with MEG. *Neuroreport* 15(13):2089–2092.
36. Perani D, et al. (2011) Neural language networks at birth. *Proc Natl Acad Sci USA* 108(38):16056–16061.
37. Johnson MB, et al. (2009) Functional and evolutionary insights into human brain development through global transcriptome analysis. *Neuron* 62(4):494–509.
38. Peña M, Pittaluga E, Mehler J (2010) Language acquisition in premature and full-term infants. *Proc Natl Acad Sci USA* 107(8):3823–3828.
39. Peña M, Werker JF, Dehaene-Lambertz G (2012) Earlier speech exposure does not accelerate speech acquisition. *J Neurosci* 32(33):11159–11163.
40. Langston RF, et al. (2010) Development of the spatial representation system in the rat. *Science* 328(5985):1576–1580.
41. Vallortigara G, Regolin L, Marconato F (2005) Visually inexperienced chicks exhibit spontaneous preference for biological motion patterns. *PLoS Biol* 3(7):e208.
42. Mazoyer BM, et al. (1993) The cortical representation of speech. *J Cogn Neurosci* 5(4): 467–479.
43. Dubois J, et al. (2008) Mapping the early cortical folding process in the preterm newborn brain. *Cereb Cortex* 18(6):1444–1454.
44. Lin P-Y, et al. (2013) Regional and hemispheric asymmetries of cerebral hemodynamic and oxygen metabolism in newborns. *Cereb Cortex* 23(2):339–348.
45. Myers MM, et al. (2012) Developmental profiles of infant EEG: Overlap with transient cortical circuits. *Clin Neurophysiol* 123(8):1502–1511.
46. Perani D, et al. (2010) Functional specializations for music processing in the human newborn brain. *Proc Natl Acad Sci USA* 107(10):4758–4763.
47. Dehaene-Lambertz G (2000) Cerebral specialization for speech and non-speech stimuli in infants. *J Cogn Neurosci* 12(3):449–460.
48. Oostenveld R, Fries P, Maris E, Schoffelen JM (2011) FieldTrip: Open source software for advanced analysis of MEG, EEG, and invasive electrophysiological data. *Comput Intell Neurosci* 2011:156869.

Supporting Information

Mahmoudzadeh et al. 10.1073/pnas.1212220110

SI Text

Subjects. Table S1 shows the clinical features of the 12 included infants. Ten additional infants were tested. No useful functional data were obtained because of fussiness ($n = 7$); poor positioning of the probe ($n = 2$); and hair obstruction ($n = 1$).

Optical Imaging System (Functional Near-Infrared System) We used a multichannel frequency-domain based optical imaging system (Imagent; ISS) for acquiring oxygenated hemoglobin and deoxygenated hemoglobin concentration changes during the auditory stimulation task. The Imagent is a frequency-domain tissue spectrometer comprising 32 intensity-modulated laser diodes at two wavelengths ($\lambda = 690$ and 830 nm) coupled to optical fibers and four gain-modulated photomultiplier tube (PMT) detectors to collect the signal at both wavelengths separately. The modulation frequency of the laser intensity was 110 MHz, and the cross-correlation frequency for heterodyne detection was 5 kHz. The reflected light was collected in PMTs and demodulated. Its mean intensity (DC), modulation amplitude (AC), and phase were determined. The average output power of the lasers was ∼0.5 mW, and the acquisition rate of the optical system was 9.1912 Hz (approximately one sample each 110 ms).

A special probe made from soft and flexible foam (thickness = 5 mm) was designed to comfortably hold the source and detector fibers on the infant's head. A patch comprising two detectors and eight emitters (optodes) entering orthogonally to the head surface was placed on each side of the head. Each of the eight optodes contained two wavelength emitter glass fibers (690 and 830 nm). Light in these two wavelengths is differently absorbed by oxy- and deoxyhemoglobine and thus allows computing their respective concentration in the medium. The average distance between the temporal cortex and the scalp is ∼7 mm in premature infants. Because the light penetration depth is about half of the distance between sources and detectors, we designed a round-grid layout, keeping a distance of 15 mm between them (Fig. S1). This layout allowed 10 points of measures (called channels thereafter), which are simultaneously sampled on each hemisphere.

Experimental Procedure. Stimuli were binaurally presented at a comfortable hearing level (∼70 dB) via speakers placed at the infant's feet, at a distance of 30 cm from his/her head. The infants were tested asleep at night to avoid the day light and the intense day activity of a neonatal care unit. They laid in a supine position on a comfortable pad in a dark and quiet incubator. The incubator was further defended against ambient light by dark sheets. The probe was smoothly secured to the infant's head to cover the perisylvian areas on each side with straps and foam padding (Fig. S1). The probe covered about 15 $cm^2 = 5$ (length) × 3 cm (width). For information, the interparietal distance is on average 7.8 cm at 31-wk gestational age (wGA) for a cranial perimeter of 29 vs. 9.4 cm at 41 wGA for a cranial perimeter of 35 cm (chart provided by the Collège Français d'échographie Foetale).

Because the optodes were attached to the two pieces of foam, their relative positions were fixed from subject to subject. Two anatomical markers (left and right ear points) were embedded into the probes to facilitate their correct orientations and positions and to enable the recovery of the probe orientation for data analysis. Location was checked before functional data acquisition.

The geometric layout of the optical probe and its projection on the brain mesh of an individual 30 wGA preterm infant [courtesy of P. Hüppi and J. Dubois, Department of Pediatrics, Geneva University Hospitals, Geneva, Switzerland (1)] are shown in Fig. S1. In this figure, the numbers 1–16 correspond to the light sources, and the letters A, B, C, and D correspond to the detectors. Using this notation, we denote the source-detector light channels as CH1, CH2,. . .CH20. The Yakovlean torque, a human structural characteristic bending the right hemisphere dorsally and forward relative to the left, is already observed in preterm infants (2, 3). This torque leads to a higher and steeper sylvian scissure in the right hemisphere than in the left. We therefore checked that our optodes placed relative to external landmarks were not at a different distance from the left and right posterior temporal cortices. J. Dubois measured the distance between the tragus and the higher posterior point of the sylvian fissure on MRI in 10 preterm infants (range, 26–32 wGA; mean age, 29.8 ± 1.7 wGA). This point is a robust cerebral landmark, easily observed in all subjects and hemisphere and is localized between channels 17–18 and 8–9. The distance was not correlated with age and remained stable during this period (4.4–4.9 cm), with no significant left–right asymmetries. We also measured the skull thickness on CT scan in preterm infants. At this age, it is <2 mm, and any asymmetry would have been too small to affect the measures. Thus, we can estimate that the errors of location of our points of measure relatively to the underlying cortical regions were negligible across our age range and that structural asymmetries were unlikely to affect our measures (4).

Data Processing. Oxy- (HbO) and deoxy-hemoglobin (Hb) are chromophores that absorb light at different wavelengths. The modified Beer Lambert law was applied to the two wavelengths signals (690 and 830 nm) to convert the signal intensities into relative changes in (de)oxy-hemoglobin concentration.

To reject artifacted signal, we used a *z*-score–based algorithm. Because individual features, such as thickness of skull and color of hair, affect the signal strength, the signal was first homogenized in each participant by computing a *z*-score across blocks for each channel and for each time sample. An artifact was assumed if the *z*-score was exceeding 4 during a window time-locked to the onset of the block [−5 to 25 s] in any channel. In that case, the entire time window covering a block was excised from the data for all channels.

The remaining cleaned HbO and Hb signals were band-pass filtered (0.03–0.5 Hz) using a zero-phase filter (Butterworth, order: 6) to eliminate physiological noise (e.g., slow drifts, arterial pulse oscillations). Both signals were segmented relative to the onset of each block (−5 to +25 s). A linear detrend and then a baseline correction on the 5 s preceding the onset of the block were performed on segments. Finally, the segments were averaged in each subject by condition for Hb and HbO [on average, 19, 19, and 21 blocks for standard (ST), deviant voice (DV), and deviant phoneme (DP) conditions, respectively].

Data Visualization. To visualize the location of the brain activity measured with our optical system, we used a realistic head model of a 30 wGA premature neonate, provided by J. Dubois and P. Hüppi (Department of Pediatrics, Geneva University Hospitals, Geneva, Switzerland) (see ref. 1 for a precise description of the steps to obtain a head and brain mesh from T2w magnetic resonance images). A virtual layout was applied on the head model using the same ears preauricular biomarkers as reference positions than in real infants. This model allowed determining the position of each virtual near-infrared spectroscopy (NIRS) acquisition channel relative to the preterm's brain (Fig. S1). Each pair of NIRS emitter and detector was then used to compute the optical signal propagation in the brain according to a photon migration model (5). This

step results in brain volume filling with information following the banana shape of the light propagation between emitters and each of the neighboring detectors, using the photon path modeled by the prescribed hitting density function. The obtained individual photon migration probability distributions were then combined together using a tricubic spatial interpolation step to consider the interaction between the individual distributions. For visualization purposes, the volume-based information was projected on the infant's brain areas covered by the optical probe with a color scale proportional to the amplitude of the response. We estimate to have obtained responses from the superior temporal gyrus, the supramarginal gyrus, the inferior part of the central sulcus, and the inferior frontal region comprising Broca's area, but note that some of the regions reported in brain imaging experiments using linguistic stimuli in infants (6) are missing, such as a large part of the superior temporal sulcus, the dorsolateral prefrontal region that was not covered by the probe, and the insula, which is too deep.

The mean signal obtained in each subject and each condition was averaged over the 12 infants (grand average) for [Hb] and [HbO]. At each time step (every ∼110 ms) of the sampling frequency (9.19 Hz) of these grand averages, we computed a surface-based topographic color map as described above to create a video animation of the brain activity during the duration of the stimulation.

Statistical Analysis. We downsampled the signal to 1 Hz in the studied time window (−5 +25 s) to decrease the number of measures. This downsampling does not affect the quality of the measures because the metabolic response is slow. We limited our analyses to the HbO signal because its signal-to-noise ratio is more robust than Hb (7, 8).

Habituation-recovery paradigms are based on the observation that stimulus repetition induces a decrease in neural activity (repetition suppression), whereas a sudden change causes a recovery of the neural activity in regions coding the parameter that changed (9, 10). This is observed at the macroscopic level using event related potentials (ERPs) (9) but also at the neuronal level (11, 12). Although the exact relation between neural activity and the metabolic response measured by fMRI is not completely understood, repetition affects the amplitude of the hemodynamic response and modifies its temporal characteristics (i.e., slope of the response, latency to the peak, duration of the plateau) in adults (13–16) and infants (17, 18). We thus expected a weaker amplitude and slower response in standard blocks relative to deviants blocks if preterm infants perceive the change of stimulus (18). To probe discrimination responses in our preterms, we thus considered the two parameters, amplitude and dynamics of the response, and used the following strategy.

To deal with the problem of repeated measures (20 channels × 30 time bins = 600), we had to reduce the number of points for each analysis. An elegant solution proposed by Maris and Oostenveld (19), initially for electrophysiological recordings with dense arrays of captors, is to use cluster-based statistics. However, if this type of statistics can rigorously prove that a statistical effect is observed, it may blur the location and latency of this effect because a single common point between close effects in space of time is sufficient to create a single cluster. We have thus completed this analysis by the analysis of the area under the curve (AUC) to locate the channels showing the maxima of the effects while reducing the number of measures to 20 (one by channel) in each condition.

The dynamics of the response in each condition was evaluated by determining its onset relative to baseline in each channel and its global slope on each hemisphere. Because these analyses suggested a transient response for the deviant voice condition, not captured by the previous analyses, we reexamined the amplitude differences focused on the first 6 s of stimulation. We chose this window because it is the classical latency to reach plateau in adults, and it was compatible with our preterms' hemodynamics (Fig. S1). In deviant blocks, at least one deviant trial was presented during this period and thus was expected to increase the metabolic needs.

Finally, we examined whether the younger infants already presented discrimination responses by dividing the group in two (younger and older than 31 wGA).

Below, we present our approach in more detail.

Cluster-based statistics on the amplitude of the response. To control the risk of false-positive or familywise error, due to multiple comparisons, we used nonparametric statistical tests as implemented in Fieldtrip (20), a toolbox developed in Matlab (available at http://fieldtrip.fcdonders.nl). This approach involved the following steps:

(*i*) Paired *t* tests between two conditions of interest, ST against DV condition, ST against DP condition, DV against DP condition, and left against right hemisphere, were performed at each channel (10 × 2 hemispheres) and time point (25 time points), with a threshold set at $P = 0.05$, two-tailed.

(*ii*) Channel-time points that exceeded the threshold were then grouped into connected clusters on the basis of their temporal and spatial proximity. Only the most adjacent channels were considered as neighbors, providing two neighbors by channel, except for the two most frontal channels (channels 1 and 11), which had only one posterior neighbor. Supra- and infra-sylvian channels were not considered as possible neighbors because the NIRS spatial resolution is sufficient to disentangle frontal and temporal responses, which are not expected to behave similarly. Each cluster was assigned a cluster value equal to the sum of each channel-time point *t*-value.

(*iii*) The type I error rate for the complete spatiotemporal set of channels and time points was controlled by evaluating the cluster-level statistics under the randomization null distribution of the maximum cluster value, which is obtained by the random permutations of the original conditions. Here we used the complete set of possible permutations: 4,095 corresponding to 2^{12} subjects − 1 (the original partition). The Monte-Carlo *P* value is estimated as the proportion of random partitions that result in larger cluster statistics than the observed one.

(*iv*) We report all clusters whose corrected *P* value was <0.025 (two-tailed test). For each cluster, we give the extremes of the time window and all channels present in the connected set of channels/time points, but note that it does not imply that a particular channel displayed significant difference during the entire window. For example, see channel 7 in Fig. 1: a single star is present at 10 s, but this sample is connected in time and space with channels 6, 3, 2, and 1.

AUC. The hemodynamic response can be characterized by two parameters: the amplitude and the duration of the response. Computing the AUC provides information reflecting the accumulative variation of HbO concentration during the whole stimulation period. Individual AUCs of the hemodynamic response were thus evaluated for each channel and each condition using only the positive part of the signals. For each comparison between two conditions, we evaluated the probability of a larger *t*-statistic in our observed comparison relative to the distribution of the *t*-values obtained when the complete set of random partitions of our data was used (here 4096-1). We used the Holm's method to correct our *P* value for false positives due to multiple comparisons (20 channels). In this method, the *P* values are ordered and examined in a stepwise fashion until the null hypothesis can no longer be rejected. In our case, the first significant *P* value had to be inferior to 0.05/20 (0.0025) to be accepted, and then 0.05/19 (0.0026), etc.

Evaluation of the activation dynamics. In each channel and condition, we evaluated the latency of the first sample showing a significant amplitude increase relative to the 5-s baseline noise. This eval-

uation was performed using individual signals and a statistical t test to compare the amplitude at each time point after the beginning of the auditory stimulation against the baseline mean amplitude. To determine each channel onset time significance, we used a corrected significance level at $P_{cor} < 0.0017$ (i.e., 0.05/30 time points) and report the first of at least two significant samples. We completed this analysis by an analysis of the slope of the HbO signal from onset of the auditory stimulation to maximum peak. For each subject, the slope of the HbO signal of all NIRS channels over one hemisphere was computed based on the following formula:

$$\text{Slope} = \Delta\text{HbO}/\Delta\text{time} = \left(\text{HbO}_{\text{peak}} - \text{HbO}_{\text{stim.onset}}\right)/\left(\text{time}_{\text{peak}} - \text{time}_{\text{stim.onset}}\right)$$

t test paired comparisons between the three conditions taken two by two were performed over the left and right channels averaged together on each side.

Analyses restricted to block onsets. Because the previous analysis showed a dynamic initially similar for both deviant conditions at least over the right hemisphere, we restricted our analysis of the deviant voice condition to the first 6 s of the blocks. We thus performed a paired t test between standard and deviant voice conditions on the mean signal averaged across the first six samples of the stimulation period using permutations and the Holm's method to correct for multiple comparisons across the 20 channels. As a follow-up, we examined the [DP–ST] and [DP–DV] contrasts in the channels showing a deviant voice effect in the previous analysis and in the homologous channels on the controlateral hemisphere, because voice and phonetic processing are differently lateralized in adults (21).

Comparison between youngest and oldest infants. Finally, we evaluated whether there was maturational change during our time window and separated our group in two subsets of six infants: younger and older than 31 wGA at birth (mean age at test, 29w4d vs. 31w6d GA). We used the same cluster-based statistics approach than above on the [DP–ST] difference and [DV–ST] difference. We also performed an ANOVA on the mean of the first 6 seconds of the block with age as a between-subject factor and conditions (3 levels), channels (10 levels), and hemisphere (2 levels) as within-subject factors. We finally performed analyses of the correlation between age and the discrimination responses.

1. Dubois J, et al. (2008) Mapping the early cortical folding process in the preterm newborn brain. *Cereb Cortex* 18(6):1444–1454.
2. Chi JG, Dooling EC, Gilles FH (1977) Gyral development of the human brain. *Ann Neurol* 1(1):86–93.
3. Dubois J, et al. (2008) Primary cortical folding in the human newborn: An early marker of later functional development. *Brain* 131(Pt 8):2028–2041.
4. Patil AV, Safaie J, Moghaddam HA, Wallois F, Grebe R (2011) Experimental investigation of NIRS spatial sensitivity. *Biomed Opt Express* 2(6):1478–1493.
5. Sassaroli A, Tong Y, Frederick BB, Renshaw PF, Fantini S (2006) Calculations of BOLD signals by use of NIRS photon migration hitting density functions. *Biomedical Optics, Technical Digest* (Optical Society of America, Fort Lauderdale, FL), paper ME30.
6. Dehaene-Lambertz G, Dehaene S, Hertz-Pannier L (2002) Functional neuroimaging of speech perception in infants. *Science* 298(5600):2013–2015.
7. Bortfeld H, Wruck E, Boas DA (2007) Assessing infants' cortical response to speech using near-infrared spectroscopy. *Neuroimage* 34(1):407–415.
8. Hoshi Y, Kobayashi N, Tamura M (2001) Interpretation of near-infrared spectroscopy signals: A study with a newly developed perfused rat brain model. *J Appl Physiol* 90(5):1657–1662.
9. Dehaene-Lambertz G, Dehaene S (1994) Speed and cerebral correlates of syllable discrimination in infants. *Nature* 370(6487):292–295.
10. Wacongne C, Changeux JP, Dehaene S (2012) A neuronal model of predictive coding accounting for the mismatch negativity. *J Neurosci* 32(11):3665–3678.
11. Miller EK, Gochin PM, Gross CG (1991) Habituation-like decrease in the responses of neurons in inferior temporal cortex of the macaque. *Vis Neurosci* 7(4):357–362.
12. Ulanovsky N, Las L, Nelken I (2003) Processing of low-probability sounds by cortical neurons. *Nat Neurosci* 6(4):391–398.
13. Kruggel F, von Cramon DY (1999) Temporal properties of the hemodynamic response in functional MRI. *Hum Brain Mapp* 8(4):259–271.
14. Thierry G, Ibarrola D, Démonet JF, Cardebat D (2003) Demand on verbal working memory delays haemodynamic response in the inferior prefrontal cortex. *Hum Brain Mapp* 19(1):37–46.
15. Dehaene-Lambertz G, et al. (2006) Functional segregation of cortical language areas by sentence repetition. *Hum Brain Mapp* 27(5):360–371.
16. Sigman M, Jobert A, Lebihan D, Dehaene S (2007) Parsing a sequence of brain activations at psychological times using fMRI. *Neuroimage* 35(2):655–668.
17. Dehaene-Lambertz G, et al. (2006) Functional organization of perisylvian activation during presentation of sentences in preverbal infants. *Proc Natl Acad Sci USA* 103(38): 14240–14245.
18. Dehaene-Lambertz G, et al. (2010) Language or music, mother or Mozart? Structural and environmental influences on infants' language networks. *Brain Lang* 114(2): 53–65.
19. Maris E, Oostenveld R (2007) Nonparametric statistical testing of EEG- and MEG-data. *J Neurosci Methods* 164(1):177–190.
20. Oostenveld R, Fries P, Maris E, Schoffelen JM (2011) FieldTrip: Open source software for advanced analysis of MEG, EEG, and invasive electrophysiological data. *Comput Intell Neurosci* 2011:156869.
21. Zatorre RJ, Belin P (2001) Spectral and temporal processing in human auditory cortex. *Cereb Cortex* 11(10):946–953.

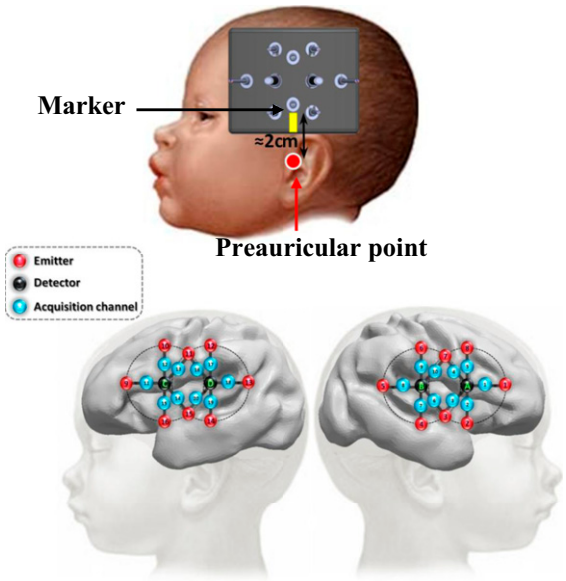

Fig. S1. (*Upper*) Schematic representation of the location of the optical probe on an infant's head relatively to anatomical landmarks. (*Lower*) Estimated projection of the optodes on the brain of a 30 wGA preterm infant [courtesy of Petra Huppi and Jessica Dubois (1)]. The eight emitters (red circles) are arranged on two 1.5-cm-diameter circles centered by the two detectors (black circles), creating 10 points of measure (channels) over each hemisphere (blue circles).

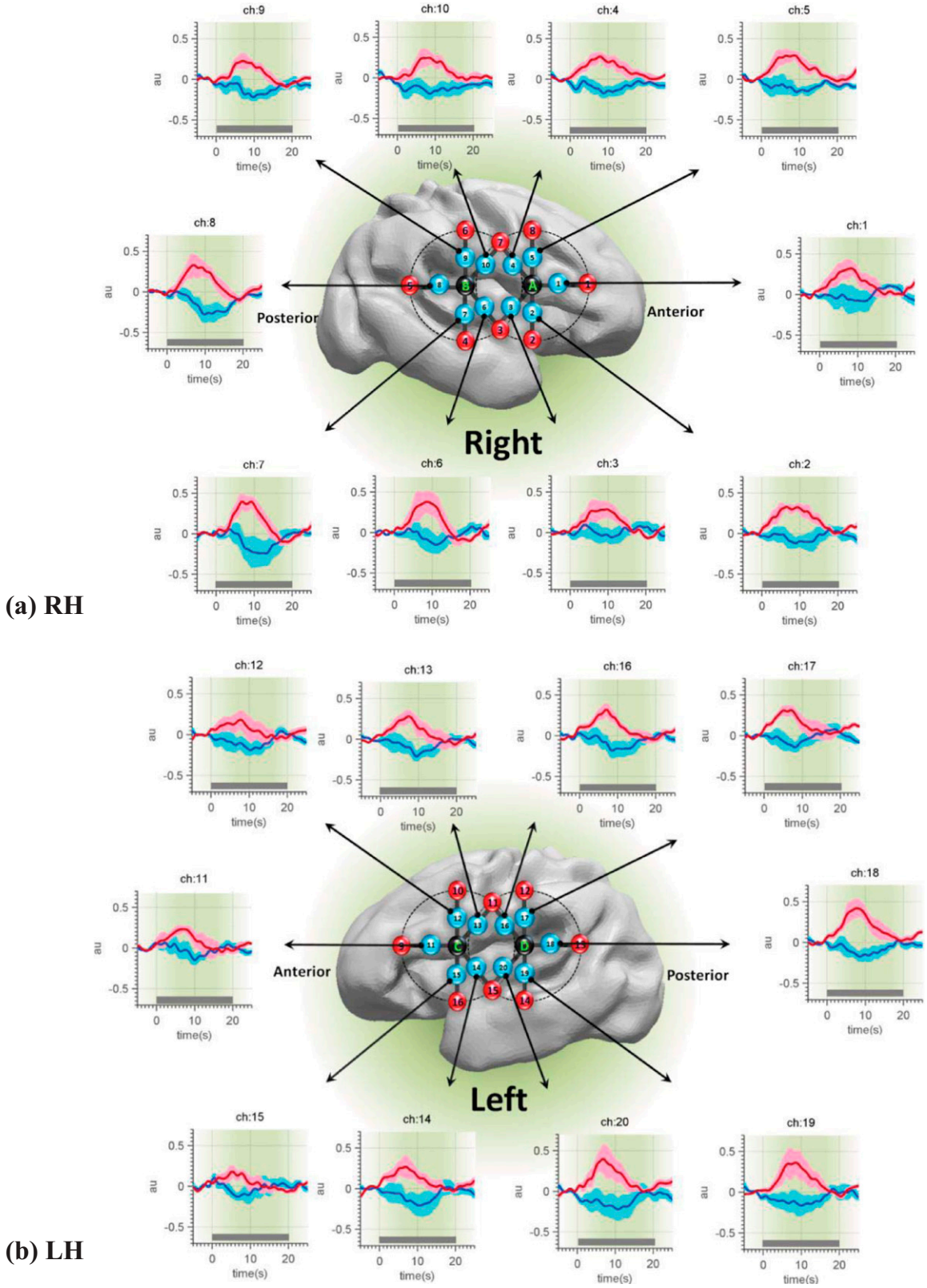

Fig. S2. Time course of the grand average of Hb (blue line) and HbO (red line) across all conditions. The *y* axis represents the concentration changes in arbitrary unit (a.u.). The *x* axis displays the time in seconds. The black rectangle bar corresponds to the duration of a block. (*A*) RH, right hemisphere; (*B*) LH, left hemisphere.

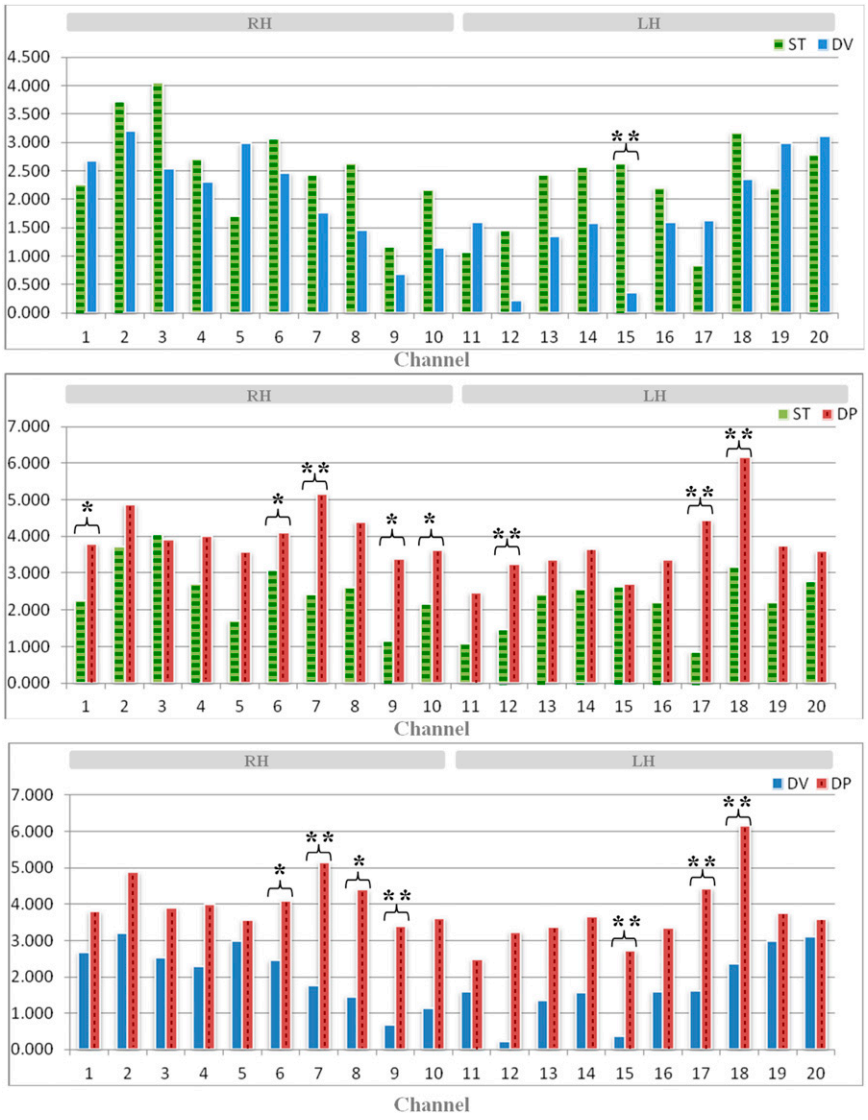

Fig. S3. AUC for the different conditions. Comparisons between conditions are performed two by two in each channel.*$P < 0.05$, **$P_{cor} < 0.05$. Channels 1–10 are over the right hemisphere (RH) and 11–20 are over the left hemisphere (LH).

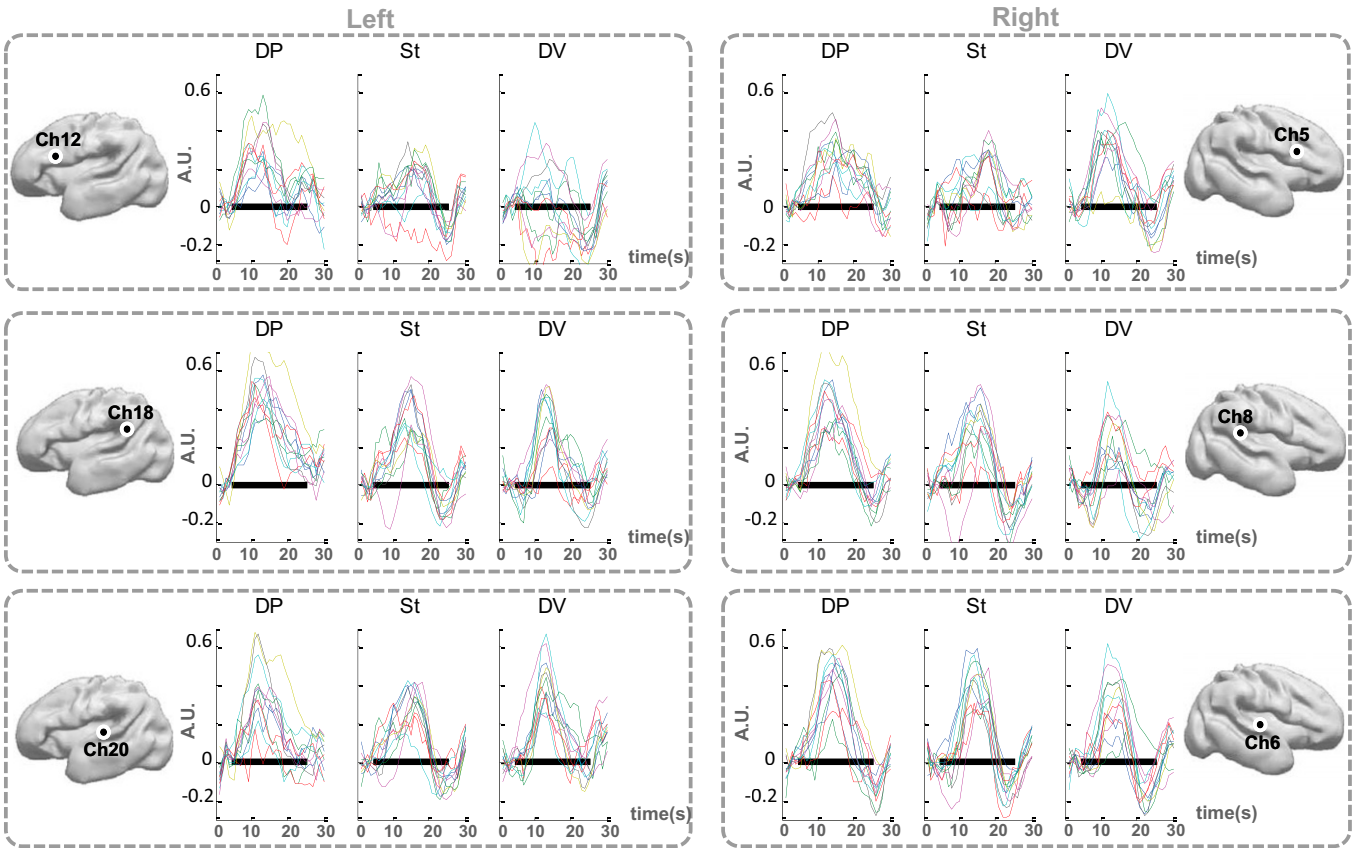

Fig. S4. Individual responses in each condition at three different locations in each hemisphere. The black rectangle corresponds to the period of stimulation (20 s). a.u., arbitrary unit.

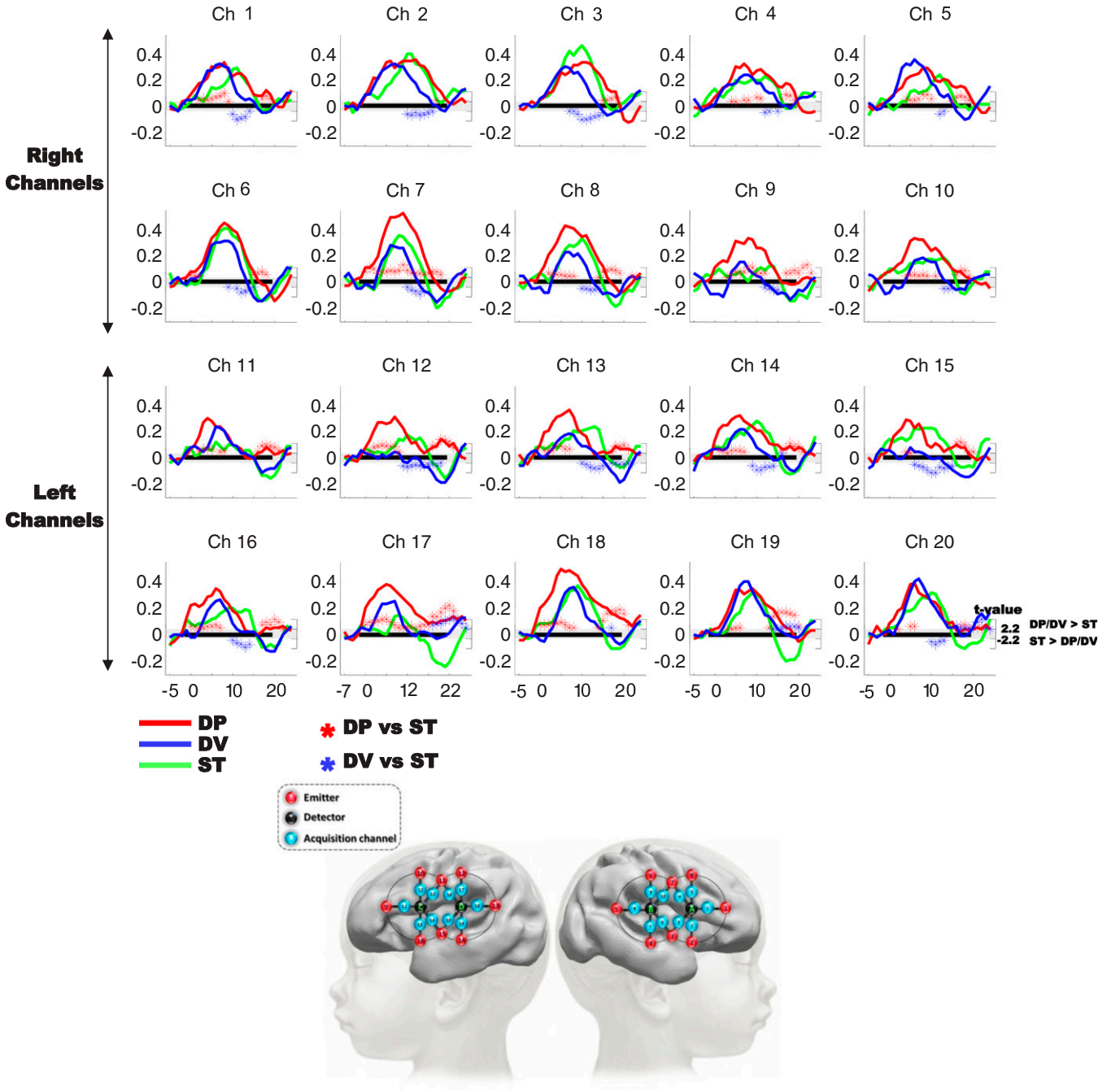

Fig. S5. Comparison of the deviant phoneme and deviant voice conditions vs. standard. The time courses of the grand average of Hb0 in deviant phoneme (DP), deviant voice (DV), and standard (ST) blocks are plotted for each channel. The black rectangle indicates the duration of the stimulation block and the stars the *t*-value of the samples (right scale) included in significant clusters as determined by a cluster-based analysis.

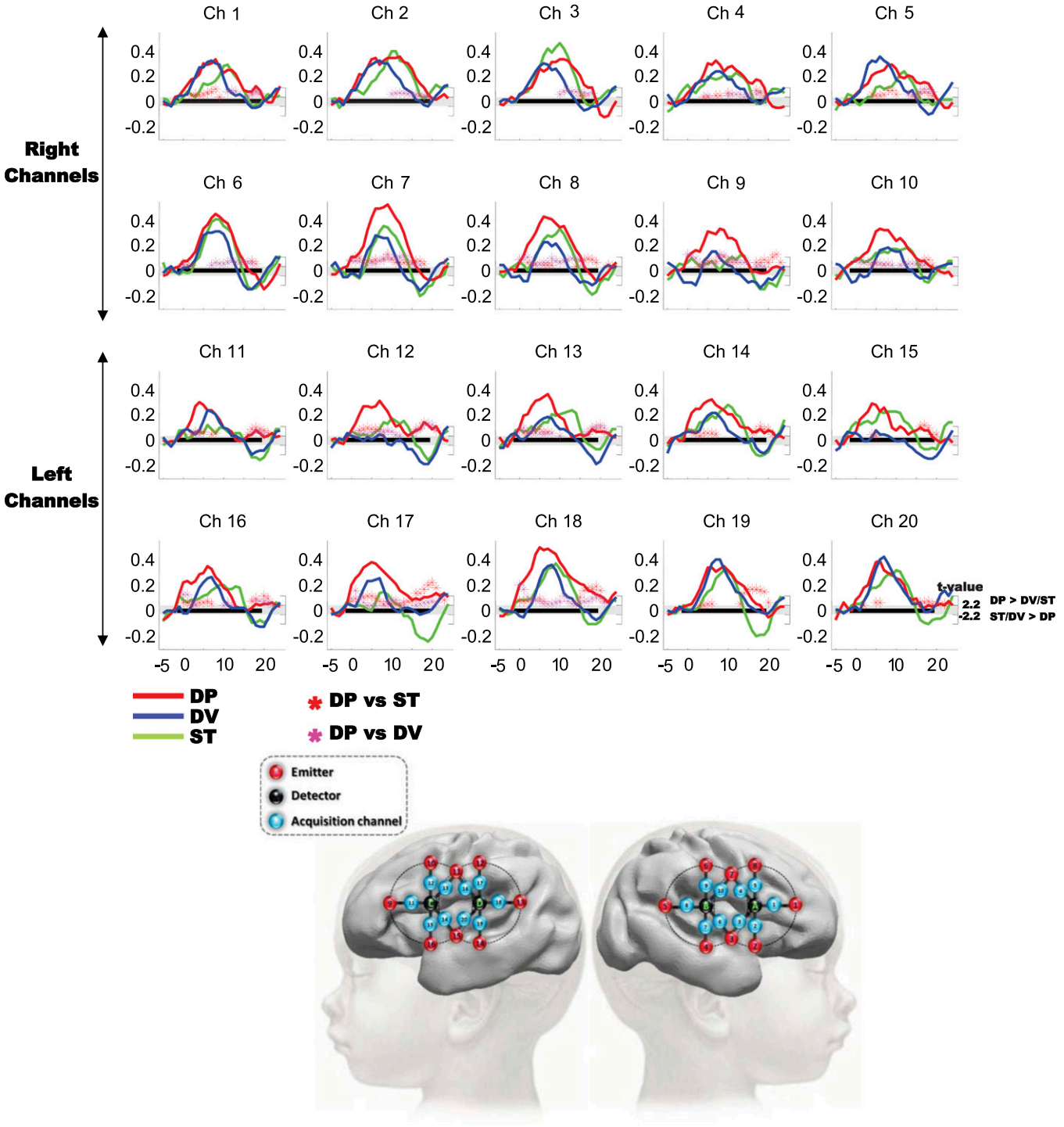

Fig. S6. Comparison of the DP condition vs. ST and DV: same legend as Fig. S4.The pink stars indicate the *t*-value of the samples (right scale) included in significant clusters as determined by a cluster-based analysis in the DP vs. DV comparison ($P_{cor} < 0.025$).

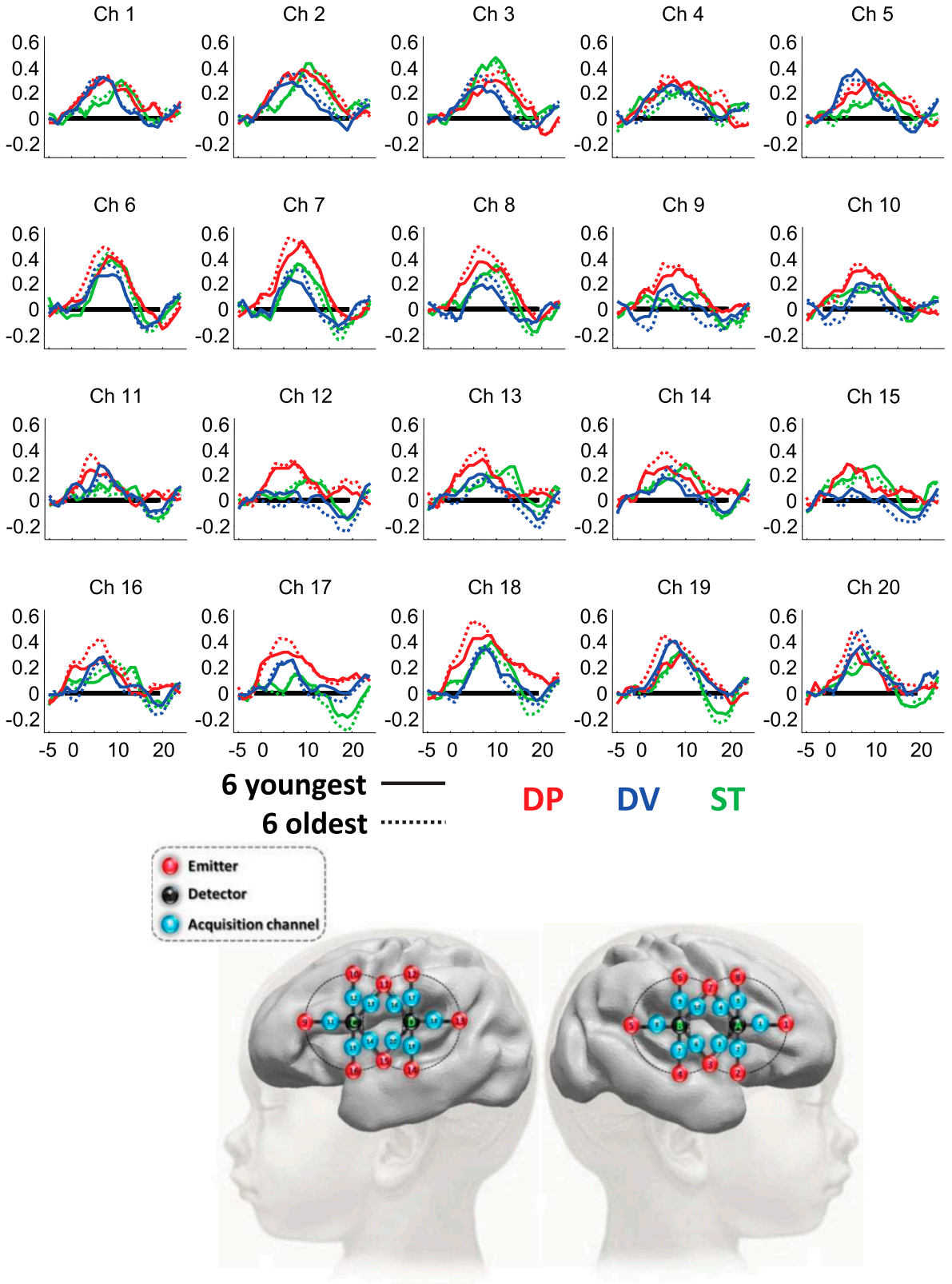

Fig. S7. Time course of the grand average of Hb0 in deviant phoneme (DP), deviant voice (DV), and standard (ST) blocks, split in function of age (mean age, 29w4d GA for the six youngest and 31w6d for the six oldest). There is no significant difference between the two groups (cluster based statistic on the whole segment). An ANOVA performed on the mean of the first 6 seconds of the block with age as a between-subject factor and conditions (3 levels), channels (10 levels), and hemisphere (2 levels) as within-subject factors did not reveal any main effect of age [$F(1,10) < 1$] nor any significant interaction of age with any combination of the other factors [$P > 0.5$, except for the triple interaction hemisphere × channel × age: $F(9,90) = 2.96$, $P = 0.004$]. The youngest group already reacted to a change of phoneme [main effect of condition: $F(1,5) = 14.6$, $P = 0.012$, condition × channel $F(9,45) = 6.57$, $P < 0.0001$] and a change of voice [main effect of condition: $F(1,5) < 1$ but condition × channel $F(9,45) = 3.72$, $P = 0.001$].

Table S1. Clinical features of the tested infants

Infant no.	Sex	GA at birth (wk)	GA at test (wk)	Birth weight (g)	EEG	Apgar (1 min)	Apgar (5 min)	Brain US	Delivery	Presentation	Clinical conditions (etiology)
1	M	32	32 2/7	1,530	N	9	7	N	Vaginal	Transverse	Twin
2	F	28 1/7	28 5/7	1,490	N	9	10	N	Cesarian	Cephalic	RPH
3	M	32	32 2/7	1,550	N	0	6	N	Cesarian	Cephalic	Preeclampsia
4	M	32	32 3/7	2,300	N	10	10	N	Vaginal	Cephalic	PROM
5	M	30 6/7	31 1/7	990	N	8	9	N	Cesarian	Cephalic	Preeclampsia
6	F	31	31 4/7	1,260	N	10	10	N	Cesarian	Cephalic	Preeclampsia
7	F	31	31 2/7	1,560	N	8	10	N	Cesarian	Breech	Anoxo-ischemia
8	M	29	29 6/7	1,610	N	10	10	N	Vaginal	Cephalic	Twin, Preeclampsia, PROM
9	M	31 1/7	31 4/7	2,300	N	10	10	N	Vaginal	Breech	Twin
10	F	28	28 3/7	995	N	8	8	N	Vaginal	Cephalic	Twin, Preeclamsia
11	M	28	28 4/7	760	N	7	10	N	Cesarian	Cephalic	Preeclampsia
12	M	30 2/7	30 5/7	1,440	N	9	10	N	Vaginal	Cephalic	PROM, Chorioamniotis

Brain US, brain ultrasonography; F, female; M, male; N, normal; PROM, premature rupture of membranes; RPH, retroplacental hematoma.

Table S2. Post hoc analyses of frontal responses during the first 6 s of stimulation in preterms divided relative to their birth age (inferior or superior to 31 wGA)

Channel	<31 wGA		≥31 wGA	
Right Ch 5 (DV vs. ST)	$F(1,5) = 10.8$	$P = 0.022$	$F(1,5) = 10.44$	$P = 0.023$
Left Ch 12 (DP vs. ST)	$F(1,5) = 8.5$	$P = 0.036$	$F(1,5) = 6.9$	$P = 0.047$
Ch 5 vs. Ch 12 * DP vs. DV	$F(1,5) = 7.9$	$P = 0.037$	$F(1,5) = 5.79$	$P = 0.061$

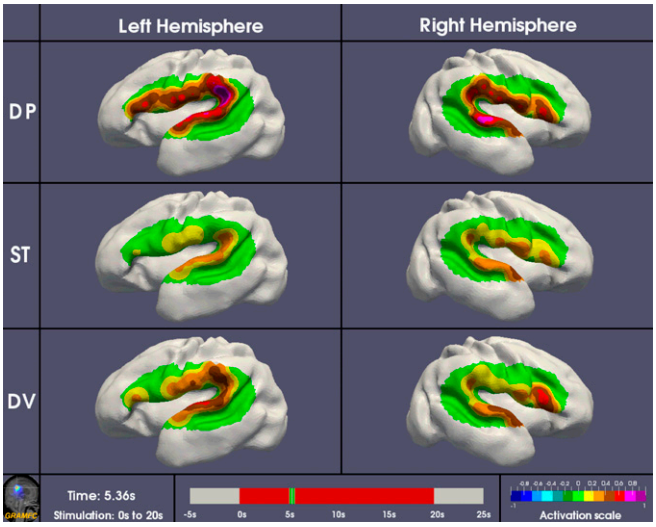

Movie S1. Infant's hemodynamic response in the three types of blocks. The red rectangle indicates the time window during which auditory stimuli were presented to infants.

Movie S1